Heliyon 7 (2021) e08619

Contents lists available at ScienceDirect

Heliyon

journal homepage: www.cell.com/heliyon

Research article

Alteration of high alkaline and alkaline basaltic rocks: parent rocks in the Lava Durian orchard, Sisaket Province, NE Thailand

Vimoltip Singtuen [a,*], Sirinthorn Phajan [a], Apussorn Anumart [a], Burapha Phajuy [b], Kantapong Srijanta [a], Sarunya Promkotra [a]

[a] Department of Geotechnology, Faculty of Technology, Khon Kaen University, 123 Mitrparp Rd., Nai Muang, Muang Khon Kaen, Khon Kaen 40002 Thailand
[b] Department of Geological Sciences, Faculty of Science, Chiang Mai University, 239 Huai Kaew Rd., Suthep, Muang Chiang Mai, Chiang Mai 50200 Thailand

ARTICLE INFO

Keywords:
Basalt
Nephelinite
Olivine basalt
Iddingsite
Hydrothermal
Geochemistry
Mineralogy

ABSTRACT

Lava Durian Sisaket is the first geographically identified (GI) fruit related to the volcano in Thailand and distributed in three districts of Sisaket Province, the southernmost edge of the Khorat Plateau. The parent rocks of orchards are important for the description of soil and rock relation with respect to mineralogical and geochemical characteristics. This work aims to study lithology, mineralogy, and geochemistry of basaltic rocks, parent rocks of in situ soil in these orchards, and delineate the existing basaltic soil models. The several orchards are covered by reddish-brown to brown in situ soils, weathered from mafic volcanic rocks: porphyritic olivine basalt, vesicular olivine basalt, and nephelinite. The microscopic image analysis, XRD, and MiniSEM-EDS are used to classify mineralogy, while XRF and analysis of large and rare elements in ICP-MS/ICP-OES were used to determine parental rocks geochemistry and alteration. The olivine basalts comprise forsterite microphenocrysts associated with bytownite, diopside, augite, pigeonite, and ilmenite groundmass, while nephelinite is composed of nepheline groundmass and bytownite-labradorite, diopside, augite, pigeonite, and ilmenite crystals. In addition, these basalts display high alteration rates, especially olivine highly altered to iddingsite. According to the geochemical data, Sisaket's basalts were identified as alkali basalt and nepheline basanite with high LILEs and LREEs (La, Nd, Pr, Gd, Eu). The kaolinite, smectite, and illite are altered from felsic minerals, while the chlorite and iddingsite are from mafic minerals. The mineralogical analyses classified secondary phyllosilicates related to low-moderate temperature hydrothermal fluid, very high cation exchange capacity (H^+, K^+, Ca^{2+}, Mg^{2+}), and tropical weathering. The alkaline and high alkaline basalts, presenting as parent rocks, are one of the parameters that produced good nitisal soil of Sisaket's agricultural areas.

1. Introduction

Basalt (mafic volcanic rock) primarily comprises plagioclase and pyroxene, alternatively consisting of other mafic minerals (olivine, magnetite) and apatite and volcanic glass. These minerals can be altered to various phyllosilicates, including clay minerals, serpentine, montmorillonite, chlorite, etc. This alteration may result from multiple internal and external factors: temperature, pressure, pH, rainwater, or other mechanisms. Basaltic soils can significantly increase the quantity and quality of agricultural produce (Bryant, 1983; Straaten, 2002; Cristan, 2003; Zhu et al., 2016).

Many countries have spatial management of basaltic soil for agriculture, producing unique products, such as coffee on the Bolaven Plateau in Laos, oranges in Brazil, grape in Australia, and good quality fruit in Japan. Most of the basalt in Thailand erupted during the Cenozoic Era, or less than 66.4 million years, which was a continuation of the Indian and Eurasian Plateaus (Barr and Macdonald, 1981. Yan et al., 2018), divided into three main groups: (1) Basanitoid basalt, a deep-molded rock by partial melting of the mantle and rapidly rising to the earth's surface, (2) Hawaiiitic basalt formed by thin melting, and (3) Tholeiitic basalt, formed by high-rate partial melting of the mantle in low pressure. Cenozoic Basalt is widely distributed in many provinces such as Lampang, Phrae, Phetchabun, Ubon Ratchathani, Chanthaburi, Trat, Rayong, Kanchanaburi, Nakhon Ratchasima, Ubon Ratchathani, Buriram, and Sisaket (Barr and Macdonald, 1981; Charusiri, 1989; Intasopa, 1993; Intasopa et al., 1995; Sutthirat et al., 1994; Boonsoong et al., 2011; Barr and Macdonald, 1981; Barr and James, 1990). Geological and metallurgical data of these basalt rocks are alkaline basalt with some

* Corresponding author.
E-mail address: vimoltipst@gmail.com (V. Singtuen).

https://doi.org/10.1016/j.heliyon.2021.e08619
Received 24 September 2021; Received in revised form 10 November 2021; Accepted 14 December 2021

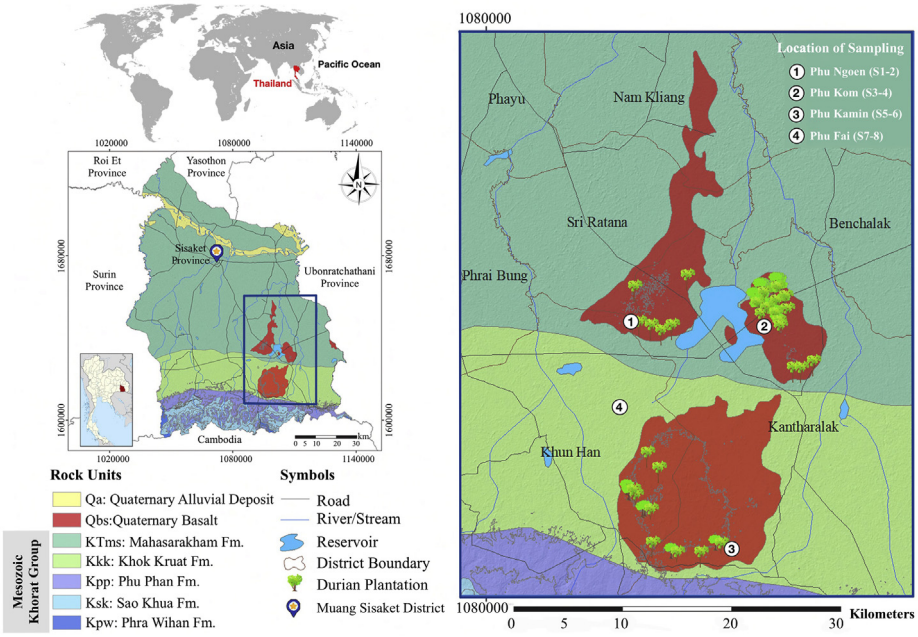

Figure 1. Geologic map of the high potential Lava Durian orchard, Sisaket Province, NE Thailand.

xenoliths (Barr and Macdonald, 1978, 1981; Yan et al., 2018). Many areas in the mentioned province have various spatial arrangements, especially the land development covered by the in situ basaltic soil to cultivate essential cash crops.

Sisaket Province is outstanding in horticultural agriculture, especially the Lava Durian Sisaket, the first geographically identified fruit of Sisaket Province in Thailand and globally (Department of Intellectual Property (DIP), 2018). Lava Durian Sisaket is characterized by firm texture, delicate, smooth with little fiber, sweetness just right, and the smell is not very pungent. This Lava Durian is classified as a famous fruit profitable for farmers by domestic trade and export to China and other regions. The Lava Durian orchards are distributed in three districts, Khun Han, Kantharalak, and Si Ratana, a rolling area covered with basalt and red soil caused by in situ weathering such rocks.

According to the durian, an economic crop that gives more income than other fruits, some agriculturists try to plant durian in many areas. However, durian present differently grows up in various soil types, parental rocks in the orchards are engaging in the study, especially Lava Durian in Sisaket. Based on the general geochemical data of previously studied basalt rocks, basalt in Sisaket province should have additional geochemical information for describing alteration minerals-related soils. Therefore, this research will support such information to be complete the lithological and mineralogical characteristics of parental rocks of in situ soil in durian orchards through alteration processes. In addition, the results of mineral alteration can be applied to explain the relationship of geochemical characteristics to stationary weathered soil. According to need more agricultural area, this study compares geochemical data with other areas covered by the same parental rocks with high tremendous agricultural areas of Sisaket.

1.1. Geologic setting

Sisaket is located on the southernmost edge of the Khorat Plateau, near Thailand and Cambodia's boundary, part of the Mainland Southeast Asia (MSEA) region. There are three main types of rock units: Quaternary alluvial deposit, Quaternary basalt, and Mesozoic sedimentary rocks of Khorat Group (Figure 1). Quaternary alluvial deposit (Qa) distributed in the northern flank of Sisaket, produced by the Mun River that flows from the northwestern side to the southeastern side and will be joined with the Chi River in Ubon Ratchathani. Almost 90% of Sisaket province is conformably covered by the Cretaceous strata (Khorat Group), consisting of Phra Wihan, Sao Khua, Phu Phan, Khok Kruat, and Mahasarakham Formations (Pholprasit and Rattanacharurak, 1979).

The Phra Wihan Formation comprises well-sorted, rounded, fine-coarse grained, pale yellow sandstone, thin-bedded siltstone, mudstone, and conglomerate. Thick sandstone beds were deposited in a braided stream environment, whereas thinner sandstone beds were deposited in meandering rivers (Meesook, 2000). Hahn (1982) indicated this formation was deposited during Late Triassic to Early Jurassic by Palynomorphs, which consists of *Ballosporites hians, Calamospora sp., Classopollis sp., Cyathidites sp., Monosuleites sp., Ballosporites sp., Cyclotriletes subgranulatus MADL, Minutosaccus sp., Lycopodiacidites sp., Chasmatosporites sp.,* and *Anulatizonites sp.*

The Sao Khua Formation presents cyclic sequences of reddish-brown sandy mudstone interbedded with siltstone, fine-to medium-grained sandstone, and conglomerate. Meesook (2000) described that sand and gravels were deposited in meandering rivers and swamps on the riverbank in semi-arid paleoclimate. In addition, plant remains of *Sphenoptheris goeppati* are dated from the Late Jurassic to Early Cretaceous by Kon'no and Asama (1973).

The Phu Phan Formation shows rounded and poorly sorted medium-to coarse-grained light grey sandstone and conglomerate (white quartz, grey-green volcanic rocks, and dark-colored chert) with large planar and trough cross-bedding. Meesook (2000) described that the Phu Phan Formation deposited in braided streams and meandering rivers of hot and humid to semi-arid environment. The deposit age is confirmed by palynomorphs that Early Cretaceous age (Racey et al., 1994, 1996).

The Khok Kruat Formation comprises reddish-brown to -purple clastic sedimentary rocks (sandstone, siltstone, mudstone, and conglomerate) interbedded with Gypsum lens and lamination. In addition, there are pebbly in some sandstone beds that contain reddish-brown siltstone, claystone, quartz, and the top of some mudstones present calcrete nodules. This formation was deposited in a meandering river during the paleoclimate change from the beginning semi-arid to the end arid (Meesook, 2000). The freshwater bivalves (i.e., *Pseudohyaia sp., Nipponaia carinate Kobayashi, Plicatotrigonioides subovalis Kobayashi, Plicatounio namphungensis*, and *Unio sampanoides*) in red sandstone, dated this formation as Early to Middle Cretaceous (Sattayarak et al., 1991).

The interbedded claystone, siltstone, and rock salts of the Maha Sarakham Formation were formed in salty lakes of an arid climate

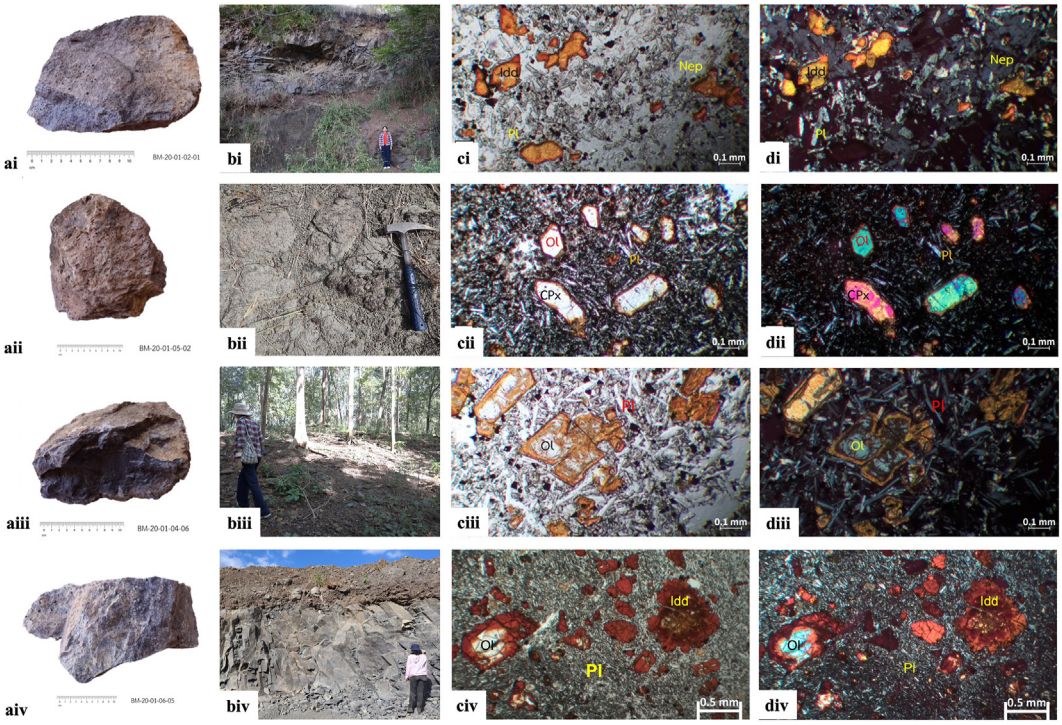

Figure 2. Basalt samples **(a)** hand specimen, **(b)** outcrop and in situ float rock, **(c)** photomicrograph in plane-polarized light, and **(d)** photomicrograph in cross-polar (Ol: olivine, Pl: plagioclase, Nep: nepheline, Px: pyroxene, Idd: iddingsite) **i:** Nephelinite in Phu Ngoen, **ii:** Vesicular (Olivine) basalt in Phu Kom, **iii:** Porphyritic (Olivine) basalt in Phu Kom, and **iv:** Porphyritic (nephelinite) basalt in Phu Kamin areas (all figures were taken by the 1st and 2nd authors; ci-ii, di-ii modified from Singtuen and Phajan, 2021).

(Meesook, 2000). Sattayarak et al. (1991) studied the Pleomorphs that indicated the age of the Maha Sarakham Formation is Cenomanian (1991). Based on data obtained from the exploration of potash deposits and petroleum, it is suggested that this formation should not be included in the Khorat Group (Sattayarak and Suteethorn, 1983; Sattayarak, 1985).

Quaternary basalts generally exploded and intruded through the Khrok Kruat and Mahasarakham formations (Jungyusuk and Sirinawin, 1983; Department of Mineral Resources DMR, 2007). These basalts erupted as sheet flows, eruptions, conical hills, and bottlenecks (cones and plugs) in four areas, consisting of Phu Ngoen, Phu Kom, Phu Kamin, and Phu Fai. Barr and Macdonald (1978, 1981) grouped these basalts into Sodic types by Eq. (1). On the other hand, the Phu Fai diabase was classified as mugearite and Phonotephrite that intruded during 3.28 ± 0.28 ma (Barr and Macdonald, 1981; Sutthirat et al., 1994).

$$Na_2O - 2.0 \geq K_2O \qquad \text{(equation 1)}$$

2. Methodology

Lava Durian orchards are distributed in three districts of Sisaket Province, which comprise Sri Ratana, Khun Han, and Kantharalak Districts. These areas can be groups into three parts of volcanic exploded as shown in red symbol in Figure 1: Phu Ngoen, Phu Kom, and Phu Kamin. Phu Ngoen is the most extended area in the north-covered Sri Ratana District. Phu Kom is a minor volcanic flow in the most eastern part of Kantharalak, while Phu Kamin is the largest in the south (Khun Han). This work studies mineralogy and geochemistry of parental rocks in the Lava Durian orchards of three main areas and Phu Fai Intrusion as the fourth area. Field observation is the first step of this study for collecting geological data, including location, outcrop description, soil stratigraphy, and sampling. The fresh and weathered rocks were collected for studying at the laboratory (Figure 1) for classifying texture, mineral composition, rock name, and alteration feature. Petrographically study analyzed thirty-two fresh rocks, which consist of eight samples from each area. Meanwhile, the photomicrographs were taken by ZEN core Imaging Software, linking ZEISS imaging and microscope solutions at the Department of Geotechnology, Khon Kaen University.

Fresh and weathered rocks were prepared by making powder samples (200 microns) from finely selected rock chips to identify chemical characteristics, specific rock names, and alteration processes. Eight representative samples with the least-altered were selected for geochemical analysis: Phu Ngoen (S1-2), Phu Kom (S3-4), Phu Kamin (S5-6), and Phu Fai (S7-8). The major elements (SiO_2, TiO_2, Al_2O_3, Fe total as Fe_2O_3, MnO, MgO, CaO, Na_2O, K_2O, and P_2O_5) were analyzed by Phillip-Magix Pro PW 2400 Wavelength Dispersive X-Ray Fluorescence spectrometer (XRF) at the Department of Geological Sciences, Chiang Mai University. The parameters consisted of an Rh-tube with a LiF 200 crystal (elemental range of K–Ru), scintillation and flow proportion detectors, and an X-ray tube operated at 60 kV with 125 mA current at a maximum power level of 4 kW. The net (background corrected) intensities were subsequently measured and calculated against calibrations derived from seven international standard reference materials (AGV-2, BCR-2, BHVO-2, BIR-1, DNC-1, GSP-2, and W-2). The SUPER Q 3.0 program was applied using inter-elements matrix corrections. The reporting detection limit was about 0.001% for major oxides and 3 ppm for trace elements. The accuracy and precision of most of the elements were better than 5%. A major oxides analysis was conducted from fusion disc samples. Meanwhile, the loss on ignitions (LOIs) was measured by sample powder in platinum crucible heating in a furnace at 1000 °C for 12 h at the Department of Architecture, Khon Kaen University. In addition, the Sodium Peroxide Fusion combined Inductively Coupled Plasma Mass Spectrometer (ICP-MS) and Inductively Coupled Plasma Optical Emission Spectrometer (ICP-OES) were used for analyzing trace elements (Rb, Sr, Zr, Y, Nb, Ni, Cr, V, Sc, Hf, Th, and Ta) and rare earth elements (La, Ce, Pr, Nd, Sm, Eu, Gd, Tb, Dy, Ho, Er, Tm, and Yb) at the SGS-CSTC Standards Technical Services Co., Ltd., China.

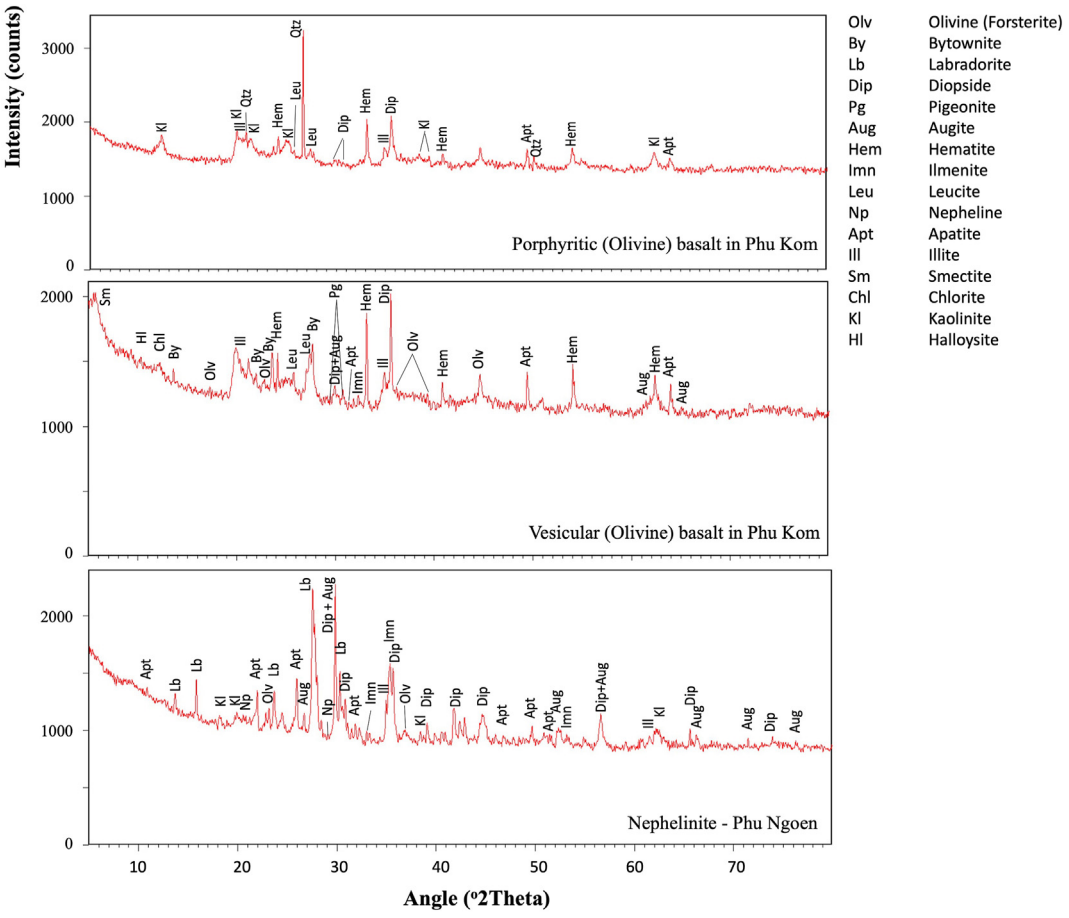

Figure 3. Mineralogy data of altered basalts by X-ray diffraction analysis (XRD) analysis. The bars below the diffraction pattern are mineral phases and corresponding diffractions (all figures were drafted by the 1st and 3rd authors).

Moreover, mineralogical analyses of moderately weathered rocks comprise two methods studied at the Faculty of Science, Khon Kaen University. Fifteen samples were analyzed by the X-Ray Diffraction (XRD), and twelve samples were diagnosed by the MiniSEM-EDS (Desktop Scanning Electron Microscopy and Energy Dispersive X-Ray Spectroscopy for classifying secondary and associated minerals. The powder samples were diffracted in the measuring range 2Theta ranging between 2^{o} to 70^{o}. The PANalytical-XRD model EMPYREAN, using $CuBiX^{3}$ sources at a wavelength, v = 1.54056Å with Small Angle X-ray Scattering (SAXS) through the Diffrac Plus and X'pert plus Programs used for analyzing qualitative minerals. In addition, the MiniSEM-EDS Model SEC (SNE-4500M) magnifies up to 100,000x with variables (5kV–30kV) used for analyzing microtexture and measuring chemical compositions of minerals. This MiniSEM-EDS was set SE detector with 4-hole variable aperture (200um, 100um, 50um, 30um), 5-axis manipulator including tilt-axis control and X, Y-axis about 40mm/R-axis: 360°. Small cubic-like samples for SEM are mounted on gold stubs (12 mm or 25 mm diameter) using conductive sticky pads, and preparation may take only hours to a few days before analysis.

2.1. Petrography and mineralogy

The petrographic study classified the basement of the in-situ soil in the lava Durian orchards as olivine basalt and nephelinite (Figure 2). Both basaltic rocks show brownish-red weathered surfaces with highly alteration rate (Figure 2a), especially olivine. Nephelinites always exploded as the bottom layer under Olivine basalts (Figure 2b).

Olivine basalts demonstrate aphanitic, porphyritic, and vesicular textures with holocrystalline, showing equigranular crystals (Figure 2c-d). Microphenocrysts (21.19 modal%) consist of 13.79 modal% subhedral olivines (0.05–0.20 mm in size), highly altered to iddingsite. In addition, 13.79 modal% clinopyroxene exhibits subhedral crystals 0.12–0.25 mm in length, and 2.67 modal% subhedral unidentified mafic minerals completely altered to iddingsite. The groundmass is 78.81% by modal, consisting of anhedral-subhedral plagioclase with albite twin, olivine, clinopyroxene, and opaque mineral.

Nephelinites presents porphyritic and vesicular textures with holocrystalline, showing equigranular crystals (Figure 2c-d). The florets consist of plagioclase, olivine, clinopyroxene, dark mineral, and opaque minerals. The phenocrysts were approximately 57.79% by modal, consisting of 21.65 modal% subhedral plagioclase (0.025 mm) with albite twin. There are also subhedral olivine phenocrysts (0.20 mm) 10.17% by modal that exhibited alteration at the margin to iddingsite. In addition, 4.76 modal% of clinopyroxene phenocrysts exhibit subhedral crystals (0.0175 mm in size) with highly altered to iddingsites, and 8.65 modal% subhedral unidentified mafic minerals (0.02–0.10 mm) completely altered to iddingsite. On the other hand, opaque mineral phenocrysts show subhedral crystals, 0.01–0.02 mm in size, 12.56 % by modal. The groundmass is approximately 42.21% by modal, consisting of nepheline, 0.275–0.320 mm in size.

Olivine basalts are mainly composed of plagioclase in rank labradorite-bytownite (An_{66-85}), with minor forsterite, ilmenite, and clinopyroxene (diopside, augite, and pigeonite series) as shown in Figure 3. Furthermore, nephelinites are composed mainly consist of plagioclase (bytownite-anorthite, An_{81-94}) and nepheline, associated with forsterite, diopside, augite, pigeonite, and ilmenite. According to XRD analysis, primary minerals of fresh and altered basalts are similar and agreeable with petrographic data. Many phyllosilicates are altered

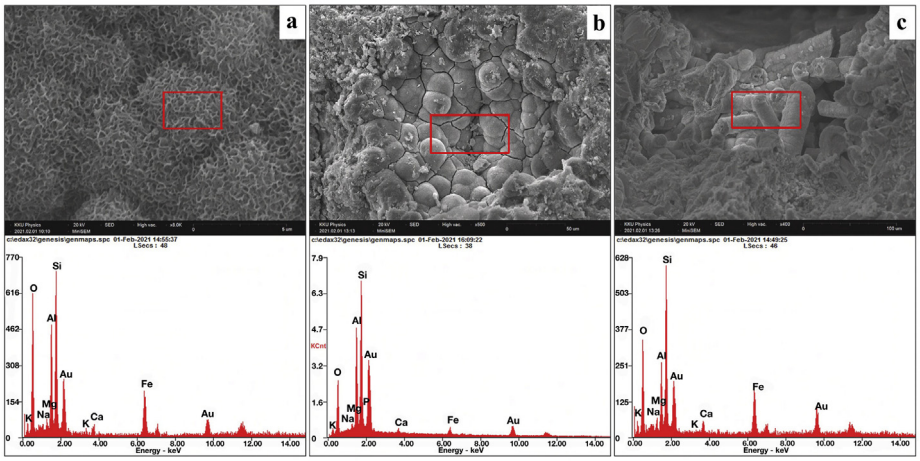

Figure 4. Scanning electron microscopy (SEM) images and geochemical data by Energy Dispersive X-ray Spectrometer (EDS) of altered basalts **(a)** nontronite with honeycomb texture, **(b)** spheroidal crystals of halloysite, and **(c)** pristine halloysite nanotubes (all figures were created and analyzed by the 1st author).

Table 1. Whole-rocks analysis for major oxides, trace elements, and REEs of studied basalts and their comparisons.

Major Oxides (wt%)	Sisaket								Buriram		Phetchabun[1]			Chanthaburi[2,3]	
	S1	S2	S3	S4	S5	S6	S7*	S8*	B1	B2	P1	P2	P3	C1	C2
SiO_2	48.75	43.81	46.54	48.25	47.26	47.24	50.87	48.52	53.52	55.26	48.48	51.99	58.64	39.90	42.00
TiO_2	1.29	1.71	1.40	1.30	1.45	1.44	1.65	1.47	2.64	2.45	2.72	0.91	0.78	3.17	2.55
Al_2O_3	17.87	16.06	17.62	17.74	17.62	17.60	19.88	17.98	15.6	15.82	15.28	18.76	18.64	11.80	11.70
Fe_2O_3	7.32	9.98	11.25	8.32	9.02	9.02	6.33	6.98	9.79	9.44	14.91	10.43	6.56	6.60	11.90
MnO	0.07	0.04	0.08	0.10	0.06	0.07	0.04	0.12	0.08	0.07	0.24	0.08	0.12	0.20	0.20
MgO	**11.07**	**10.32**	**9.81**	**10.82**	**9.91**	**9.90**	**5.62**	**9.76**	**5.76**	**5.49**	**4.89**	**6.26**	**3.64**	**9.10**	**8.70**
CaO	7.94	10.17	7.63	8.16	8.93	8.93	7.19	8.07	6.70	7.05	7.75	8.39	7.26	10.00	10.00
Na_2O	2.56	4.01	2.31	3.35	3.78	3.84	3.63	3.46	1.73	1.81	4.08	2.50	3.80	5.10	3.50
K_2O	**2.64**	**2.25**	**2.79**	**1.47**	**1.08**	**1.09**	**3.20**	**2.94**	**1.48**	**1.31**	**1.3**	**0.54**	**0.53**	**1.20**	**0.90**
P_2O_5	0.48	1.66	0.57	0.49	0.88	0.89	0.83	0.69	0.88	0.74	0.38	0.14	0.21	1.10	1.01
LOI	1.62	2.35	1.22	1.77	2.67	2.63	1.78	1.51	1.83	0.82	1.55	2.39	1.50	4.10	4.40
Trace Elements REEs (ppm)															
La	28.20	85.90	31.00	30.10	52.40	50.30	34.20	27.90	25.80	25.80	12.30	5.00	9.60	69	-
Pr	6.42	17.50	6.76	7.02	10.80	10.10	9.11	7.31	7.86	7.86	4.20	1.60	2.90	-	-
Nd	24.60	64.20	26.3	27.30	40.40	36.60	36.60	29.10	34.70	34.70	24.00	9.00	14.70	66	-
Eu	2.10	4.10	2.05	2.17	2.90	2.64	2.75	2.27	2.83	2.83	1.95	0.86	0.95	-	-
Gd	4.89	10.10	4.90	4.80	6.65	6.36	6.42	5.39	6.34	6.34	6.29	2.79	3.83	-	-
Tb	-	-	-	-	-	-	-	-	-	-	1.16	0.55	0.50	-	-
Dy	3.94	6.06	4.03	4.29	4.98	4.63	4.55	3.77	4.56	4.56	6.67	3.32	2.84	-	-
Ho	0.71	0.95	0.71	0.68	0.81	0.80	0.73	0.67	0.73	0.73	1.39	0.63	0.56	-	-
Er	-	-	-	-	-	-	-	-	-	-	3.52	1.77	1.36	-	-
Tm	28.20	85.90	31.00	30.10	52.40	50.30	34.20	27.90	0.22	0.22	0.52	0.29	0.22	-	-
Yb	1.30	1.30	1.20	1.20	1.40	1.30	1.20	1.00	1.20	1.20	3.51	2.09	1.65	-	-
Ce	51.10	147.00	54.60	51.50	90.20	82.80	68.30	54.70	54.40	54.40	31.1	10.80	21.3	150	-
Sm	6.70	13.30	5.50	7.80	9.20	8.30	8.60	7.80	9.90	9.90	6.26	3.16	3.21	-	-
Th	4.20	8.20	4.00	3.80	6.20	6.00	3.60	3.10	2.30	2.30	6.40	6.70	6.70	9	-
Ta	4.50	7.40	4.40	3.80	5.70	6.00	3.60	3.70	2.80	2.80	-	-	-	-	-
Nb	52.00	109.00	57.00	50.00	77.00	72.00	50.00	44.00	41.00	41.00	6.1	<2	609	98	106
Zr	168.00	239.00	176.00	174.00	191.0	190.00	212.00	177.00	205.00	205.00	185	87	142	365	369
Hf	4.00	6.00	4.00	4.00	4.00	4.00	5.00	5.00	5.00	5.00	3.96	1.75	2.51	-	-
Y	21.40	29.90	21.90	19.50	22.50	21.70	22.90	18.50	18.90	18.90	44.7	24	26	32	32

[1] Boonsoong et al. (2011).
[2] Barr and Macdonald (1981).
[3] Barr and James, 1990.
* Basaltic rocks (shallow intrusion) with non-agricultural areas.

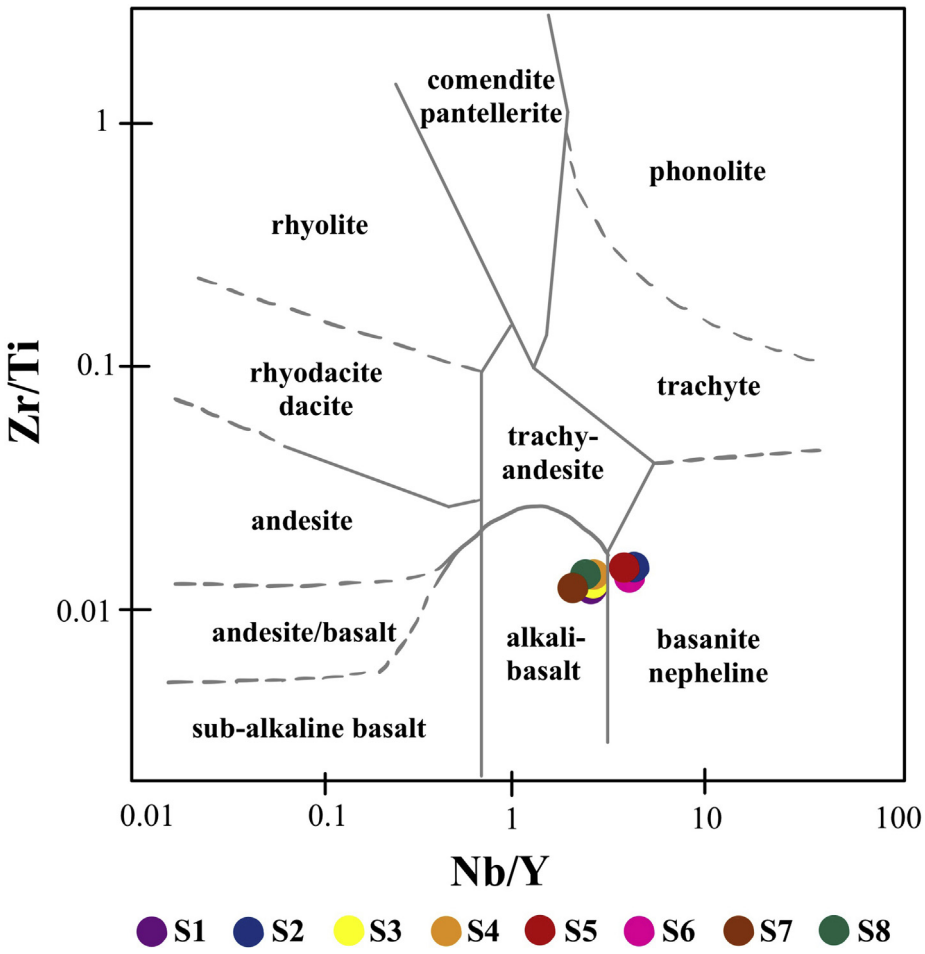

Figure 5. Plot of Zr/TiO_2 against Nb/Y for the basaltic rocks in Sisaket Province (diagram modified from Winchester and Floyd, 1997; Singtuen and Phajan, 2021). Diagram illustrates Sisaket basalts consisting of alkali basalt (sample S1 S3 S4 S7 S8) and nepheline basanite (sample S2 S5 S6) (figure was analyzed and modified by the 1st and 2nd authors).

from basalts as secondary minerals consisting of the Kaolin group (i.e., kaolinite, nacrite, halloysite, dickite), illite, clinochlore, nontronite stevensite, rectorite, sauconite, chamosite, allophane, as well as epidote (Figure 3). The crystallinity of the illite is generally rich in the olivine basalts. The l0- Å peak shows partial overlap to the 12- Å peak indicating illite to illite-smectite interstratification (Wilson, 1987). The kaolinite crystallinity is generally poor, with XRD patterns typically showing a broad *d* (001) reflection at 7.2–7.4 Å, often with distinct asymmetry towards the low-angle side, and a broad d (002) peak at 3.6 Å. All altered basaltic rocks demonstrate similar quantitative of secondary halloysite (the peaks from 7 to 11) and quartz, as shown in Figure 3. The weathered basalts present 0.79–2.81% kaolinite and very high intensity in porphyritic basalt. In addition, nephelinite shows 1.13 illite, while olivine basalt presents 5.78% illite, 2.84% smectite, 0.37% chlorite, and a small amount of halloysite. Based on the petrographic data of Singtuen and Phajan (2021), Phu Kom vesicular basalts present a high rate of alteration by the percentage of iddingsite, which is alteration production of olivine. Thus, this basalt demonstrates a high number of secondary minerals in XRD analysis. The replacement secondary Kaolin group (i.e., nontronite halloysite) always has honeycomb texture, spheroidal crystals, and pristine nanotubes (Figure 4).

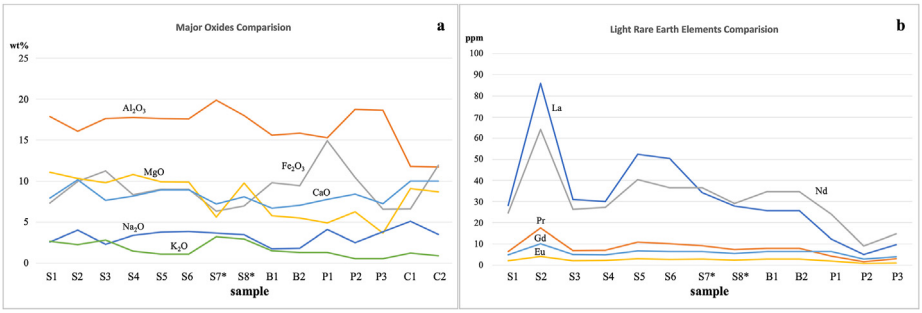

Figure 6. Geochemical Comparision between Sisaket Basalts and basalt from other areas where plant Durian (a) major oxides comparison and (b) light rare earth elements (LREEs) comparison (Boonsoong et al., 2011; Barr and Macdonald, 1981; Barr and James, 1990; Singtuen and Phajan, 2021) (all figures were analyzed and created by the 1st and 2nd authors).

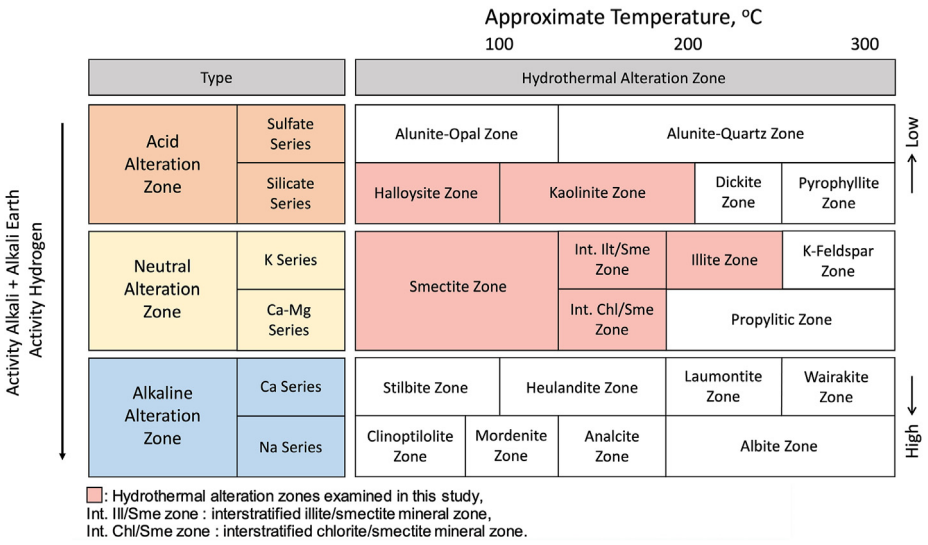

Figure 7. The diagram shows mineralogical changes by fluid pH, salinity, and temperature (modified from Utada, 1980; Kohno and Maeda, 2012). The ratio of cations/H^+ along with the temperature of hydrothermal fluids dictates the mineral assemblage formed. Altered studied basalts present secondary minerals: halloysite, kaolinite, smectite, illite, and chlorite (red field) (figure was analyzed and created by the 1st author).

2.2. Geochemistry

Geochemical data comprise major oxides, trace elements, and rare earth elements (REEs) are demonstrated in Table 1. Sample S1–S6 were collected from the Lava Durian orchard in Sri Ratana, Khun Han, and Kantharalak Districts. Sample S7 and S8 are shallow mafic intrusion (higher SiO_2 and low MgO) from the Phu Fai area with no agricultural area.

The basaltic rocks that are source rocks of in situ soil in the Lava Durian orchard present 43.81–48.75 wt% SiO_2, 17.87–16.06 wt% Al_2O_3, 7.32–9.98 wt% Fe_2O_3, 9.81–11.07 wt% MgO, 7.63–10.17 wt% CaO, 2.56–4.01 wt% Na_2O, 1.08–2.79 wt% K_2O, and 0.48–1.66 wt% P_2O_5. Furthermore, trace elements of Sisaket basaltic rocks demonstrate the significant difference, especially Zr, Ti, Nb, and Y. The ratio of Zr/TiO_2 and Nb/Y follows the diagram of Winchester and Floyd (1997) in Figure 5 classified the basaltic rocks in Sisaket Province into two groups: alkali basalt (sample S1 S3 S4 S7 S8) and nepheline basanite (sample S2 S5 S6) that generated from difference alkaline magma series (Singtuen and Phajan, 2021).

Thus, Sisaket basalts are highly alkaline and alkaline volcanic rocks, presenting prominent large ion lithophile elements (alkaline and alkaline earth) and LREEs (La, Nd, Pr, Gd, Eu). These LILE and LREE contents are different from basalts from other famous Durian orchards in Buriram, Phetchabun, and Chanthaburi provinces that present only alkaline basaltic rocks (Boonsoong et al., 2011; Barr and Macdonald, 1981; Barr and James, 1990), as shown in Figure 6. Additionally, trace elements are challenging to compare with other basalts, especially Chanthaburi basalts that lack these data.

2.3. Mineral alteration

An experimental study by Bowen in 1928 revealed that the crystallization sequence of basalt constituents is olivine, pyroxene, and calcic plagioclase. However, basalt is also composed of other minerals, such as apatite, spinel, magnetite, amphibole, or mafic volcanic glass. Each mineral has a different crystallization temperature range based on its chemical properties. Most of the high-temperature crystallized mafic igneous compounds are readily weathering and altering on the earth's surface. Due to pressure, temperature, humidity, pH that causes the exchange of ions within the rock mass or with the external environment (Fowler and Zierenberg, 2016), especially olivine, is converted to serpentine, chlorite or iddingsite. It has the most remarkable alteration rate within the rock as temperature and pH change (Chen and Brantley, 2000; Hänchen et al., 2006; Pokrovsky and Schott, 2000; Rosso and Rimstidt, 2000; Wogelius and Walther, 1991). The pyroxene has a secondary alteration rate to chlorite in conditions where the factors are similar (Chen and Brantley, 1998; Knauss et al., 1993; Oelkers and Schott, 2001).

The hydrothermal alteration can be divided into 15 more specific zones by mineral assemblages (Figure 7). Classification of hydrothermal alteration zones based on temperature and activity ratio of aqueous cation species in the hydrothermal solution has been described by Utada (1980). According to mineralogical analyses by the microscope, MiniSEM-EDS, and XRD, secondary minerals include halloysite, kaolinite, smectite, illite, and chlorite. Three alteration types are classified as low-to moderate-temperature (<250 °C) of hydrothermal fluids: (1) acid with H^+ activity caused to halloysite and kaolinite zone, (2) neutral zone with K activity cause to smectite and illite zone, and (3) neutral zone with Ca + Mg activity that makes smectite and chlorite zone. Therefore, the hydrothermal fluids of volcanic activities and rifting structures affected these in situ soils in Sisaket Lava Durian Orchards. In addition, the XRD patterns present quartz crystals in high counts, which are unreasonable with alkaline magma; thus, quartz occurs as secondary minerals (i.e., hydrothermal alteration, pore filling, replacement).

The altered Sisaket basalts consist of many kinds of mafic minerals, including forsterite (Mg_2SiO_4), pigeonite [$(Ca_xMg_yFe_z)$ $(Mg_yFe_z)Si_2O_6$], diopside ($CaMgSi_2O_6$), and augite [$(Ca_xMg_yFe_z)$ $(Mg_yFe_z)Si_2O_6$]. According to petrography (alteration rim) and XRD analysis, these mafic minerals altered to secondary minerals such as chlorite (clinochlore $[(Mg,Fe^{2+})_5Al(Si_3Al)O_{10}(OH)_8]$ and chamosite $[Fe^{2+}, Mg,Fe^{3+})_5Al(Si_3Al)O_{10}(OH,O)_8]$. In addition, nontronite is the iron (III) rich member of the smectite group formed in weathered basalts, precipitation of iron, and silicon-rich hydrothermal fluids (Bischoff, 1972; Eggleton 1975) according to secondary quartz (silica remain from hydrothermal crystallization).

Moreover, the plagioclase with high calcium can alter to epidote, sericite, or another clay mineral depending on its chemical composition and related factors (Chou and Wollast, 1985; Gudbrandsson et al., 2014; Knauss and Wolery, 1986). Therefore, Sisaket basalts contain both bytownite and labradorite series $[(Na,Ca)\ (Al,Si)_4O_8]$ can be altered to secondary minerals; rectorite $[(Na,Ca)Al_4(Si,Al)_8O_{20}(OH)_4 \cdot 2(H_2O)]$, such as illite $[(K,H_3O)\ (Al,Mg,Fe)_2(Si,Al)_4O_{10}\ [(OH)_2{\cdot}(H_2O)$ and smectite (nontronite $[(CaO_{0.5},Na)_{0.3}Fe_3^{2+}(Si,Al)_4O_{10}(OH)_2{\cdot}nH_2O]$). The rectorite and dickite are phyllosilicate clay minerals and essential alteration

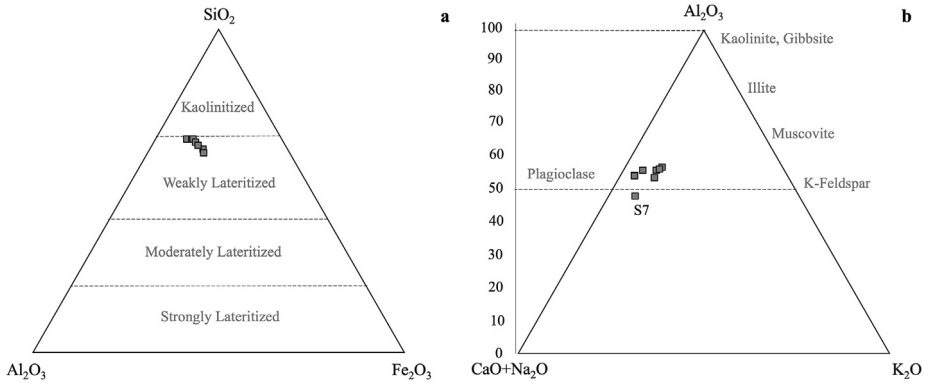

Figure 8. (a) Triangular plot of SiO_2–Fe_2O_3–Al_2O_3 showing degree of lateritization (after Schellmann, 1986). (b) A–CN–K ternary diagram (modified from Nesbitt and Young, 1982; Fedo et al., 1995) showing weathering trends of basaltic rocks (all figures were analyzed and created by the 1st author).

indicators in hydrothermal systems and soils (Moore and Reynolds, 1997). Meanwhile, epidote is commonly found in regionally low to moderate grade metamorphosed rocks related to hydrothermal alteration.

Furthermore, the nepheline ($Na_3KAl_4Si_4O_{16}$) is prone to alteration to zeolites (especially natrolite), sodalite, kaolin, or compact muscovite (Spencer, 1911; Nesse, 2000). However, Sisaket basalts demonstrate secondary minerals altered from nepheline, comprising kaolinite ($Al_2Si_2O_5(OH)_4$), halloysite ($Al_2Si_2O_5(OH)_4$), and smectite group (sauconite $[Na_{0.3}Zn_3(SiAl)_4O_{10}(OH)_2{\cdot}4H_2O]$). The halloysite is polymorphous with kaolinite—these minerals are alteration products of volcanic glass and feldspars from hydrothermal processes. On the other hand, sauconite is one of the phyllosilicates in the smectite clay group, typically be genetically related to hydrothermal fluids circulation (Large, 2001; Hitzman et al., 2003; Boni and Mondillo 2015).

Additionally, if the rock contains mafic volcanic glasses, it can cause instability. As a result, the volcanic glass was altered to a clay mineral with high iron and magnesium, including kaolinite, montmorillonite, and palagonite (Gislason and Oelkers, 2003; Guy and Schott, 1989; Michalski et al., 2006; Greenberger et al., 2012; Stranghoener et al., 2018). The composition of soil, especially clay minerals (phyllosilicates), weathered and altered from basalt, results from the different chemical compositions of the original rock. These minerals can be indicated from mineralogy, which can help explain the fertility of nutrients in the primary soil that will directly affect the use in agriculture.

Major oxides can determine the degree of alteration through SiO_2, Al_2O_3, Fe_2O_3 triangular plots (Figure 8a). The decreasing relative SiO_2 contents divide alteration into three levels; weak, moderate, and robust lateritization. The kaolinization is decided by aluminum within the parental rocks, which is, to begin with, changed over to kaolinite through the combination with the accessible silica, which any encourages weathering (i.e., silica loss) past this condition, in this manner, marks the organize of the laterite.

The samples indicate that the weakly weathered basalts develop through the downward weathering process associated with kaolinization to weak lateritization (Figure 8a). According to the Al_2O_3–Fe_2O_3–SiO_2 ternary diagram by Schellmann (1986), the limit of Sisaket parental rocks is determined that these rocks occur at 66.03% SiO_2 and gradual change from SiO_2 - rich to Fe_2O_3-rich to Al_2O_3-rich compositions (Figure 8a) and of increasing degree of lateritization.

2.4. Chemical index of alteration (CIA)

Chemical changes during weathering processes, alkaline and alkaline earth ions (Na^+, K^+, Ca^{2+}, Mg^{2+}) of the parent rocks are relatively mobile, resulting in mobile elements depletion and immobile elements enrichment. The chemical index of alteration (CIA) increases from the parent rock upward to the surface soil, suggesting the increase of chemical weathering, accompanied by the conversion of feldspars to clay minerals (potassium with other alkali and alkaline earth elements combination). The extent of weathering rocks has been calculated by major oxides and alkaline elements (equation 2), presenting stoichiometric changes during weathering processes (Budihal and Pujar, 2018).

$$CIA = [Al_2O_3 / (Al_2O_3 + CaO + Na_2O + K_2O)] \times 100. \quad \text{(equation 2)}$$

The least-altered basaltic samples have an average CIA value of 56.1191, ranging from 49.4306 to 58.6431, 55.5482 in alkaline basalt, and 57.0706 in nepheline basanite, which suggest that the weathering resulted in more depletion of the labile alkalis and alkaline earth materials in nepheline basanite than alkaline basalt. Samples from the weathering profile of the study area are plotted using Al_2O_3-(CaO + Na_2O)–K_2O or A–CN–K ternary plot (Figure 8b), which demonstrates alteration trends in major element composition and minerals during the chemical weathering.

The A–CN–K triangular diagram describes the consequence of chemical weathering where plagioclase is dissolved, causing depletion of Ca, Na, and K and enrichment of Al (Nesbitt and Young, 1982; Fedo et al., 1995). As weathering progresses, plagioclase would be decomposed with further weathering and, with the releasing of K at the Al_2O_3 apex, kaolinite and halloysite are the predominant clay minerals (Budihal and Pujar, 2018). The studied rocks were slightly weathered, and the plots in Figure 8b trend to muscovite and kaolinite fields, reflecting the presence of phyllosilicate clay minerals as main mineralogical components.

3. Discussion for basaltic soil model

The dominant soils in the studied area from the Digital Soil Map of the World (FAO 2007) were described based on the "World Reference Base for Soil Resources" (FAO 2014) and the "Encyclopedia of Soil Science" (Chesworth 2008), suggesting that the area is covered by Nitisols. Nitisols are strongly weathered, deep, red, well-drained tropical soils and have a clayey subsurface horizon with blocky structural elements that crumble into polyhedric peds with shiny faces. The soil profile in Sisaket has mostly an AB(t)C horizon sequence, which presents red or reddish-brown, and is deeper than 150 cm (Elstner, 2017) that is in line with the basaltic soil model of this study (Figure 10). In addition, Elstner (2017) describes that the nitisols is one of the most fertile soils in humid tropics, which presents stable, well-drained soils with good soil structure, good porosity, adequate water holding capacity, and excellent root ability. This basaltic soil presents the cation exchange capacity (CEC) higher than other tropical soils (Ferralsols, Lixisols, and Acrisols), especially Ca^{2+} and Mg^{2+}, same as the study of Webb and Dowling (1990) that describe Tertiary basalt in central Queensland.

Thanachit et al. (2006) studied soils on a catena on Cenozoic basalt in Khon Buri, Nakhon Ratchasima province (NE Thailand). They noted that parent basalt soils under a tropical climate had produced kaolin and iron

Figure 9. Outcrops of parental rocks and in situ soil (a) post-mining area at Phu Ngoen, (b) reddish soil of durian orchard at Phu Kom, (c) weathered rocks at Phu Kom, and (d) mining outcrop near durian orchard at Phu Kamin (all figures were taken by the 1st author).

Figure 10. The model of the basaltic soil profile in the high potential Lava Durian orchard, Sisaket Province, NE Thailand (figure was analyzed and created by the 1st author).

oxide minerals as the dominant soil materials similar to Sisaket weathered parental rocks. The high amounts of Mg, Ca, and K derived from basalt weathering, and leached ions accumulation crystallize to smectite and carbonate, agreeable with Millot (1970).

Alkaline basalts and nepheline basanite are associated with altered basalts and scoria as parent rocks of in situ soil in Lava Durian orchards. The outcrops of Phu Ngoen and Phu Kom are located near the post-mining area where local people plant durian, while durian orchard is at Phu Kamin nearby the active quarry (Figure 9). These rocks are composed of high #Ca plagioclase (labradorite to anorthite), high #Mg olivine (forsterite) presented as microphenocrysts. Groundmass phases consist of clinopyroxene (diopside-pigeonite-augite) and ilmenite as well as nepheline in basanite. Some pores and fractures of vesicular basalts are replaced by secondary quartz, which may be formed by hydrothermal alteration.

Moreover, the eruption ages of these volcanic rocks have resulted in alteration rates. The basalts in Lava Durian Orchards were older than the Phu Fai Diabase erupted during 3.28 ± 0.28 ma and older than Cenozoic basalts in others of Thailand (Barr and Macdonald, 1981; Sutthirat et al., 1994). Thus Sisaket's basalt is highly altered to in situ soil more than others and can produce good soil with high nutrients from the chemical composition of parent rocks. Furthermore, Sisaket demonstrates structural geology such as fault, joint, and fold that can be factors of alteration and weathering.

The model of the basaltic soil profile from orchards nearby the post-mining area in Phu Ngoen presents the thick layer of reddish-brown to brown soil approximately 50 cm associated with organic matter as O-horizon on the top (Figure 10). Topsoil or A-horizon dept 1.5–2.0 m below humus layer and comprise reddish soil with basaltic gravels. Many layers of altered basalts, scoria, alkali basalt, and nepheline basanite are

associated as strata rank between medium to thick layers. Geochemical data demonstrate that the studied basalts have very high alkaline, alkaline earth, light rare earth elements (LREEs), especially K_2O and MgO. Both alkaline basalts and nepheline basanites present high alteration rates and similar secondary minerals, including Kaolin group (kaolinite, nacrite, halloysite, dickite), illite, clinochlore, nontronite stevensite, rectorite, sauconite, chamosite, allophane, and epidote. This study assumes that all clay minerals can occur in the open system of weathering and alteration processes of Sisaket basalts follow the study of Prudêncio et al. (2002) that describe clay minerals from weathered basalts comprise smectites, associated with halloysite, illite, and palygorskite. They also mentioned that kaolin minerals prevail in topographic highs, while smectites predominate in lower areas that can evolve either to palygorskite or analcime. The intensive basalt weathering resulted in the formation and abundance of kaolinite and halloysite clay minerals as well as the iron oxide in the strongly weathered soil (Asio and Jahn, 2007).

4. Conclusion

The Lava Durian Orchards are distributed in Sisaket Province: Khun Han, Kantharalak, and Si Ratana districts. According to petrography, the studied rocks in three areas were porphyritic olivine basalt, vesicular olivine basalt, and nephelinite. Geochemical data classified these basalts as alkali basalt and nepheline basanite according to high alkaline (K^+), alkaline earth (Ca^{2+}, Mg^{2+}), and LREEs. The alkali basalt and nepheline basanite illustrate have very high CEC during weathering and alteration processes. The mineralogical changes suggest many secondary phyllosilicates related to low-moderate temperature hydrothermal fluid and cation (H^+, K^+, Ca^{2+}, Mg^{2+}) activities and general weathering process in the tropical climate. The chlorite group and iddingsite altered from forsterite and clinopyroxene, while high #Ca plagioclase altered to illite and smectite group. In addition, nepheline can be altered to kaolinite, halloysite, and smectite. The basaltic soil profile by field investigation demonstrates a thick layer of reddish-brown to brown in situ soil (nitisols) overlay on the alkaline and high alkaline basalts as well as scoria and altered basaltic rocks. Therefore, high alkaline and alkaline earth basalts are one of the parameters that produced the high nutrient soil of Sisaket's orchard. However, the rock's alteration rate by eruption age, structural geology, and hydrothermal fluids also affected the soil quality and quantity.

Declarations

Author contribution statement

Vimoltip Singtuen: Conceived and designed the experiments; Performed the experiments; Analyzed and interpreted the data; Contributed reagents, materials, analysis tools or data; Wrote the paper.

Sirinthorn Phajan, Apussorn Anumart & Kantapong Srijanta: Performed the experiments.

Burapha Phajuy & Sarunya Promkotra: Contributed reagents, materials, analysis tools or data.

Funding statement

Vimoltip Singtuen was supported by Young Researcher Development Project of Khon Kean University.

Data availability statement

Data included in article/supplementary material/referenced in article.

Declaration of interests statement

The authors declare no conflict of interest.

Additional information

No additional information is available for this paper.

References

Asio, V.B., Jahn, R., 2007. Weathering of basaltic rock and clay mineral formation in Leyte, Philippines. Philippine Agric. Sci. 90, 222–230.

Barr, S.M., James, D.E., 1990a. Trace element characteristics of upper cenozoic basaltic rocks of Thailand, kampuchea and Vietnam. J. Asian Earth Sci. 4, 233–242.

Barr, S.M., Macdonald, A.S., 1978. Geochemistry and petrogenesis of late Cenozoic Alkaline basalts of Thailand. Malaysia. Bull. Geol. Soc. Malays. 10, 25–52.

Barr, S.M., Macdonald, A.S., 1981. Geochemistry and geochronology of late Cenozoic alkaline basalts of Southeast Asia. Geol. Soc. Am. Bull. 92, 1069–1142.

Bischoff, J.L., 1972. A ferroan nontronite from the Red Sea geothermal system. Clay Miner. 20, 217–223.

Boni, M., Mondillo, N., 2015. The Calamines and the Others: the great family of supergene nonsulfide zinc ores. Ore Geol. Rev. 67, 208–233.

Boonsoong, A., Panjasawatwong, Y., Metparsopsan, K., 2011. Petrochemistry and tectonic setting of mafic volcanic rocks in the Chon Daen–Wang Pong area, Phetchabun, Thailand. Isl. Arc 20, 107–124.

Bowen, N.L., 1928. The Evolution of the Igneous Rocks. Princeton University Press, New Jersey.

Bryant, J.P., 1983. Fertilizer Minerals. Industrial Minerals and Rocks, 1. The Society of Mining Engineers, New York.

Budihal, R., Pujar, G., 2018. Major and trace elements geochemistry of laterites from the Swarnagadde plateau, uttar Kannada district, Karnataka, India. J. Geosci. Geomat. 6 (1), 12–20. http://pubs.sciepub.com/jgg/6/1/2.

Charusiri, P., 1989. Lithophile Metallogenic Epochs of Thailand: Geological and Geochronological Syntheses. Ph.D. Thesis, Queen's University, Kingston, p. 819.

Chen, Y., Brantley, S.L., 1998. Diopside and anthophyllite dissolution at 25° and 90°C and acid pH. Chem. Geol. 147 (3-4), 233–248.

Chen, Y., Brantley, S.L., 2000. Dissolution of forsteritic olivine at 65°C and 2 < pH < 5. Chem. Geol. 165 (3-4), 267–281.

Chesworth, W., 2008. Encyclopedia of Soil Science. Springer, New York.

Chou, L., Wollast, R., 1985. Steady-state kinetics and dissolution mechanisms of albite. Am. J. Sci. 285 (10), 963–993.

Cristan, C.A., 2003. Success in Brazil with Citrus and Omamentals. Remineralize the earth's online Magazine.

Department of Intellectual Property (DIP), 2018. The Registration of Geographical Indication Sisaket Lava Durian No. 61100112 (in Thai). Bangkok, Department of Intellectual Property.

Department of Mineral Resources (DMR), 2007. Geologic map of Sisaket Province (scale 1: 1,000,000). Department of Mineral Resources. http://www.dmr.go.th/download/pdf/NorthEast/srisaket.pdf.

Eggleton, R.A., 1975. Nontronite topotaxial after Hedenbergite. Am. Mineral. 60, 1063–1068.

Elstner, P., 2017. Soils of Mainland Southeast Asia. Chiang Mai: Warm Heart Foundation. Available: https://www.echocommunity.org/en/resources/b3026a7c-8e7c-4b37-b920-d60117438e19.

FAO, 2007. Digital Soil Map of the World (2007-02-28). Version 3.6, 1:5.000.000 scale. FAO, Rome. Available: http://www.fao.org/geonetwork/srv/en/metadata.show?id=14116.

FAO, 2014. World Reference Base for Soil Resources. Updated 2015, World Soil Resources Report 106. Rome: FAO. Available: http://www.fao.org/3/a-i3794e.pdf.

Fedo, C.M., Nesbitt, H.W., Young, G.M., 1995. Unraveling the effects of potassium Metasomatism in sedimentary rocks and paleosols, with implications for paleoweathering conditions and provenance. Geology 23, 921–924.

Fowler, A.P.G., Zierenberg, R.A., 2016. Elemental changes and alteration recorded by basaltic drill core samples recovered from in situ temperatures up to 3458C in the active, seawater-recharged Reykjanes geothermal system. Iceland. Geochem. Geophys. Geosyst. 17, 4722–4801.

Gislason, S.R., Oelkers, E.H., 2003. Mechanism, rates, and consequences of basaltic glass dissolution: II. An experimental study of the dissolution rates of basaltic glass as a function of pH and temperature. Geochem. Cosmochim. Acta 67 (20), 3817–3832.

Greenberger, R.N., Mustard, J.F., Kumar, P.S., Dyar, M.D., Breves, E.A., Sklute, E.C., 2012. Low temperature aqueous alteration of basalt: mineral assemblages of Deccan basalts and implications for Mars. J. Geophys. Res. 117, E00J12.

Gudbrandsson, S., Wolff-Boenisch, D., Gislason, S.R., Oelkers, E.H., 2014. Experimental determination of plagioclase dissolution rates as a function of its composition and pH at 22 °C. Geochem. Cosmochim. Acta 139, 154–172.

Guy, C., Schott, J., 1989. Multisite surface reaction versus transport control during the hydrolysis of a complex oxide. Chem. Geol. 78 (3-4), 181–204.

Hahn, L., 1982. Stratigraphy and marine ingressions of the mesozoic Khorat group in northeastern Thailand. Geol. Jahrb. 43, 7–35.

Hänchen, M., Prigiobbe, V., Storti, G., Seward, T.M., Mazzotti, M., 2006. Dissolution kinetics of fosteritic olivine at 90–150 °C including effects of the presence of CO_2. Geochem. Cosmochim. Acta 70 (17), 4403–4416.

Hitzman, M., Reynolds, N., Sangster, D., Allen, C., Carman, C., 2003. Classification, genesis, and exploration guides for nonsulfide zinc deposits. Econ. Geol. 98, 685–714.

Intasopa, S., 1993. Petrology and Geochronology of the Volcanic Rocks of the Central Thailand Volcanic Belt. Ph.D. Thesis, University of New Brunswick, New Brunswick, p. 242.

Intasopa, S., Dunn, T., Lambert, R.S.J., 1995. Geochemistry of Cenozoic basaltic and silicic magmas in the central portion of the Loei-Phetchabun volcanic belt, Lop Buri, Thailand. Can. J. Earth Sci. 32, 393–409.
Jungyusuk, N., Sirinawin, T., 1983. Cenozoic basalt of Thailand. In: Proceedings of the Conference on Geology and Mineral Resources of Thailand, pp. 62–70.
Knauss, K.G., Wolery, T.J., 1986. Dependence of albite dissolution kinetics on pH and time at 25°C and 70°C. Geochem. Cosmochim. Acta 50 (11), 2481–2497.
Knauss, K.G., Nguyen, S.N., Weed, H.C., 1993. Diopside dissolution kinetics as a function of pH, CO_2, temperature, and time. Geochem. Cosmochim. Acta 57 (2), 285–294.
Kohno, M., Maeda, H., 2012. Relationship between point load strength and uniaxial compressive strength of hydrothermally altered soft rocks. Int. J. Rock Mech. Min. 50, 147–157.
Kon'no, E., Asama, K., 1973. Mesozoic Plants from Khorat, Thailand: Geology and Palaeontology of Southeast Asia, 12. Tokyo University Press, pp. 149–172.
Large, D., 2001. The geology of non-sulphide zinc deposits - an overview. Erzmetall: Journal for Exploration, Mining and Metallurgy 54, 264–274.
Meesook, A., 2000. Cretaceous environment of northeastern Thailand. In: Cretaceous Environment of Asia, first ed. Elsevier Science Publishers B.V, Amsterdam, pp. 207–223.
Michalski, J.R., Kraft, M.D., Sharp, T.G., Christensen, P.R., 2006. Effects of chemical weathering on infrared spectra of Columbia River Basalt and spectral interpretations of Martian alteration. Earth Planet Sci. Lett. 248 (3–4), 822–829.
Millot, G., 1970. Geology of Clays; Weathering, Sedimentology, Geochemistry. Springer-Verlag, Heidelberg.
Moore, D.M., Reynolds, J.R.C., 1997. X-Ray Diffraction and the Identification and Analysis of Clay Minerals, second ed. Oxford University Press, Oxford.
Nesbitt, H.W., Young, G.M., 1982. Early Proterozoic climates and plate motions inferred from major element chemistry of lutites. Nature 299, 715–717.
Nesse, W.D., 2000. Introduction to Mineralogy. Oxford University Press, New York.
Oelkers, E.H., Schott, J., 2001. An experimental study of enstatite dissolution rates as a function of pH, temperature, and aqueous Mg and Si concentration, and the mechanism of pyroxene/pyroxenoid dissolution. Geochem. Cosmochim. Acta 65 (8), 1219–1231.
Pholprasit, Ch., Rattanacharurak, P., 1979. The Geologic Map Scale 1:250,000 - Sheet Chom Krasan (In Thai). Department of Mineral Resources, Bangkok.
Pokrovsky, O.S., Schott, J., 2000. Kinetics and mechanism of forsterite dissolution at 25°C and pH from 1 to 12. Geochem. Cosmochim. Acta 64 (19), 3313–3325.
Prudêncio, M.I., Sequeira Braga, M.A., Paquet, H., Waerenborgh, J.C., Pereira, L.C.J., Gouveia, M.A., 2002. Clay mineral assemblages in weathered basalt profiles from central and southern Portugal: climatic significance. Catena 49 (1–2), 77–89.
Racey, A., Goodall, J.G.S., Love, M.A., Polachan, S., Jones, P.D., 1994. New age data for the mesozoic Khorat group of northeastern Thailand. In: Proceedings of International Symposium on Stratigraphic Correlation of Southeast Asia, pp. 245–252. Bangkok, Thailand.
Racey, A., Love, M.A., Canham, A.C., Goodall, J.G.S., Polachan, S., Jones, P.D., 1996. Stratigraphy and reservoir potential of the mesozoic Khorat group, NE Thailand, Part I: stratigraphy and sedimentary evolution. J. Petrol. Geol. 19 (1), 5–39.
Rosso, J.J., Rimstidt, J.D., 2000. A high resolution study of forsterite dissolution rates. Geochem. Cosmochim. Acta 64 (5), 797–811.
Sattayarak, N., 1985. Review on geology of Khorat Plateau. Proceedings of Conference on Geology and Mineral Resources Development of the Northeast Thailand. Khon Kaen, Thailand, pp. 23–30.
Sattayarak, N., Suteethorn, V., 1983. Geologic Map of Thailand 1:500,000 (Northeastern Sheet). Department of Mineral Resources Thailand, Bangkok.
Sattayarak, N., Polachan, S., Charusirisawad, R., 1991. Cretaceous rock salt in the northeastern part of Thailand. In: Proceedings of Seventh Regional Conference on Geology, 36. Bangkok, Thailand.
Schellmann, W., 1986. A new definition of laterite. In: Lateritisation Processes, IGCP-127, 120. Geological Survey of India, Memoirs, pp. 1–7.
Singtuen, V., Phajan, S., 2021. Petrographic and geochemical data of high alkaline basalts, Sisaket terrain, NE Thailand. Data Brief 39, 107540.
Spencer, L.J., 1911. Nepheline. In: Chisholm, Hugh (Ed.), Encyclopædia Britannica, eleventh ed., 19. Cambridge University Press.
Straaten, P., 2002. Rocks for Crops. Department of Land Resource Science, University of Guelph, Canada.
Stranghoener, M., Schippers, A., Dultz, S., Behrens, H., 2018. Experimental microbial alteration and Fe mobilization from basaltic rocks of the ICDP HSDP2 drill core, Hilo, Hawaii. Front. Microbiol. 9 (1252).
Sutthirat, C., Charusiri, P., Farrar, E., Clark, A.H., 1994. New $^{40}Ar/^{39}Ar$ geochronology and characteristics of some Cenozoic basalts in Thailand. In: Proceedings of International Symposium on Stratigraphic Correlation of Southeast Asia. Bangkok, Thailand, pp. 306–320.
Thanachit, S., Suddhiprakarn, A., Kheoruenromne, I., Gilkes, R.J., 2006. The geochemistry of soils on a catena on basalt at Khon Buri, northeast Thailand. Geoderma 135, 81–96.
Utada, M., 1980. Hydrothermal alteration related to igneous acidity in Cretaceous and Neogene formations of Japan. Mining Geology Japan Special Issue 8, 67–83.
Webb, A.A., Dowling, A.J., 1990. Characterization of basaltic clay soils (vertisols) from the Oxford land system in central Queensland. Aust. J. Soil Res. 28 (6), 841–856.
Wilson, M.J.A., 1987. Handbook of Determinative Methods in Clay Mineralogy. Chapman & Hall, London.
Winchester, J.A., Floyd, P.A., 1997. Geochemical discrimination of different magma series and their differentiation products using immobile elements. Chem. Geol. 20, 325–343.
Wogelius, R.A., Walther, J.V., 1991. Olivine dissolution at 25°C: effects of pH, CO_2, and organic acids. Geochem. Cosmochim. Acta 55 (4), 943–954.
Yan, Q., Shi, X., Metcalfe, I., Liu, S., Xu, T., Kornkanitnan, N., Sirichaiseth, Th., Yuan, L., Zhang, Y., Zhang, H., 2018. Hainan mantle plume produced late Cenozoic basaltic rocks in Thailand, Southeast Asia. Nature 8 (1), 1–14.
Zhu, H., Zhao, Y., Nan, F., Duan, Y., Bi, R., 2016. Relative influence of soil chemistry and topography on soil available micronutrients by structural equation modeling. J. Soil Sci. Plant Nutr. 16 (4), 1038–1051.